

Light-powered micromotor driven by geometry-assisted, asymmetric photon-heating and subsequent gas convection

Li-Hsin Han,¹ Shaomin Wu,¹ J. Christopher Condit,² Nate J. Kemp,³ Thomas E. Milner,² Marc D. Feldman,^{4,5} and Shaochen Chen^{1,a)}

¹Department of Mechanical Engineering, The University of Texas at Austin, C2200, Texas 78712, USA

²Department of Biomedical Engineering, The University of Texas at Austin, C0800, Texas 78712, USA

³Volcano Corporation, 1 Fortune Drive, Billerica, Massachusetts 01821, USA

⁴Department of Medicine, University of Texas Health Science Center, San Antonio, Texas 78229, USA

⁵South Texas Veterans Health Care System, San Antonio, Texas 78229, USA

(Received 9 April 2010; accepted 26 April 2010; published online 27 May 2010)

We report on the design, fabrication, and analysis of a light-driven micromotor. The micromotor was created from a nanoporous polymer with close-packed gold nanoparticles which generate heat by absorbing light. The blades of the micromotor were curved, forming convex and concave sides. Upon lateral irradiation, by geometric effect the convex side transfers more photon-generated heat to the surrounding gas molecules, causing a convective motion of gas and leading to the rotation of the micromotor. The light-driven motions of gas molecules were analyzed using molecular dynamics modeling. © 2010 American Institute of Physics. [doi:10.1063/1.3431741]

Recent studies demonstrate that light is a promising power source to actuate small machines.^{1,2} Operated by the intake of photon energy and the subsequent discharge of heat, light-powered actuators require no peripheral elements to sustain mass flows or electric charges. This simple mechanism promotes system miniaturization and simple power delivery, which are important to many advanced applications for biomedical, mechanical, and aerospace engineering.³⁻⁵

Invented in the 19th century by Sir William Crookes, Crookes radiometer, also known as the light mill, was the earliest light-powered rotating machine [Fig. 1(a)].^{6,7} Crookes' light mill has a four-vanes rotor, which is asymmetrically colored; each vane of the rotor is dark on one side and bright on the other. The rotor is mounted on the tip of a needle for minimum friction and is sealed in a glass container of partial vacuum (0.1–1 Torr). Upon irradiation, the vanes rotate with the dark sides retreating from the source of light. The cause of rotating motion is gas convection induced by different rates of photon heating at the different sides of the vanes; the dark sides, which absorb more photon energy, generate more heat to the surrounding gas molecules than the bright sides. This asymmetric photon heating leads to a temperature gradient in the gas across each vane, inducing the convection of gas molecules which drives the rotation of rotor.

The principle of light mill can be applied to develop light-powered micromotors for devices in a narrow internal space. For example, for advanced cardiovascular imaging, a light mill can be installed inside a catheter (~2 mm in diameter) to drive a rotating micromirror that directs a near-infrared laser to scan the internal wall of coronary artery and receive information about the spatial distribution of cardiovascular tissues or the accumulation of atherosclerotic plaque.^{8,9} The rotation speed of the micromirror should be at least several hundreds revolutions per minute (rpm) for minimal measurement time. An electric micromotor can generate

the required rotation; however, it is undesirable to apply electricity inside the coronary arteries, for a leaked voltage or an electrostatic discharge, which is common in electric motors, can disrupt the heart. The light mill is unique for this type of application when electricity or fuel is not appropriate to power the device due to safety concerns.

However, the light mill has never been used for a micromotor but remains an educational tool for a century after being invented; in spite of the advanced technology of microelectromechanical system and nanofabrication,³⁻⁵ the original Crookes mill is hard to miniaturize; it requires patterning distinct material (optical) properties at the specific locations within a very thin, three-dimensional space.

We created a high speed, miniaturized light mill with a homogeneous optical property [Fig. 1(b)]; for the fabrication

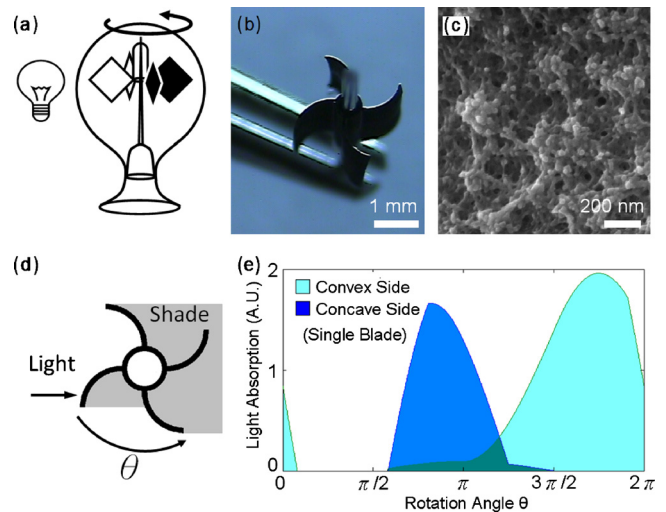


FIG. 1. (Color online) (a) Illustration of Crookes radiometer; (b) the created light mill at the tips of tweezers; (c) SEM image of closely packed gold nanoparticles on the porous light mill blade; (d) illustration of asymmetric irradiation on the light mill, which rotates in the indicated direction; and (e) simulated rates of light absorption by the convex and concave surfaces at each blade vs the light mill rotation angle θ ; integrating the areas below each curve shows an approximately doubled rate of heating at the convex side compared to the concave side.

^{a)}Author to whom correspondence should be addressed. Electronic mail: sschen@mail.utexas.edu.

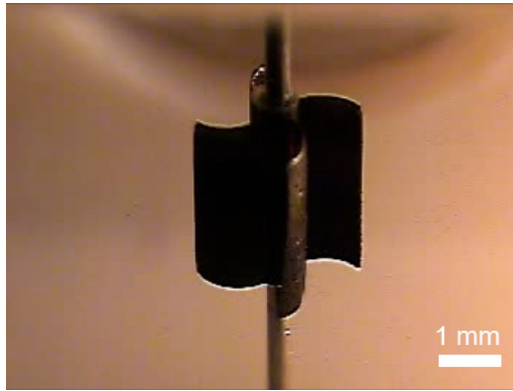


FIG. 2. (Color online) In experiments, the light mill rotates with the convex surfaces retreating from the source of lateral irradiation (enhanced online). [URL: <http://dx.doi.org/10.1063/1.3431741.1>]

process, see supplementary material, Ref. 10]. It has an axially asymmetric rotor with four blades; each blade is curved, forming a convex and concave sides. Upon lateral irradiation, this geometry causes different rates of photon heating on the two sides of the blade; the absorption by the convex side is higher than twice the absorption by the concave side [Figs. 1(d) and 1(e)]. Consequently, the convex side of the blade transfers more heat from light to surrounding gas, leading to a temperature gradient across the blade for driving the gas molecules, which force the rotor to rotate.

The rotor is uniformly coated for light absorbing. The rotor was made from a microporous polymer, which has interconnecting pores less than a micron in sizes. This polymer reacted with a precursor which produces metallic gold,¹¹ forming closely packed gold nanoparticles (diameter < 50 nm) in the micropores [Fig. 1(c)]. Coated with nanoparticles, the rotor became uniformly dark and strongly light absorbing due to electrodynamic interactions among closely packed gold nanoparticles.^{12,13} Having a large internal surface for heat transfer, the micropores with gold nanoparticles become an efficient light-powered heater for the surrounding gas molecules.

Supported by a jewel bearing in an irradiated glass vacuum chamber, the rotor spins rapidly with the convex surfaces retreating from the source of light (see Fig. 2 and accompanying online video). Data from an optical motion sensor shows that the rotation speed varied from several hundreds to thousands of rpm, depending on the light intensity and also on the degree of vacuum [Figs. 3(a) and 3(b)]. For white-light illumination, the rotation speed was maximized at about 400 mTorr, corresponding to a mean free path (MFP) of air of $130 \mu\text{m}$.¹⁴ Because the light mill ceases to spin at lower pressure, we conclude that the observed rotation does not stem from Yarkovsky effect, namely, the recoil momentum from thermally irradiated photons.¹⁵ The experiment result is, however, consistent with the calculation by Albert Einstein, who concluded that the net-force exerted on a light mill is from heat-induced gas momentum and is maximized when the MFP of surrounding gas becomes comparable to the thickness of the blades of the light mill, which is $75 \mu\text{m}$ in this case.⁶

Heat generation by the gold particulate coating is much more efficient than regular dyes. Electromagnetic modeling [Fig. 4(a)] from our previous publication demonstrates the efficiency of absorption by the closely packed nanoparticles as follows:¹⁶ while individual gold nanoparticles absorbs

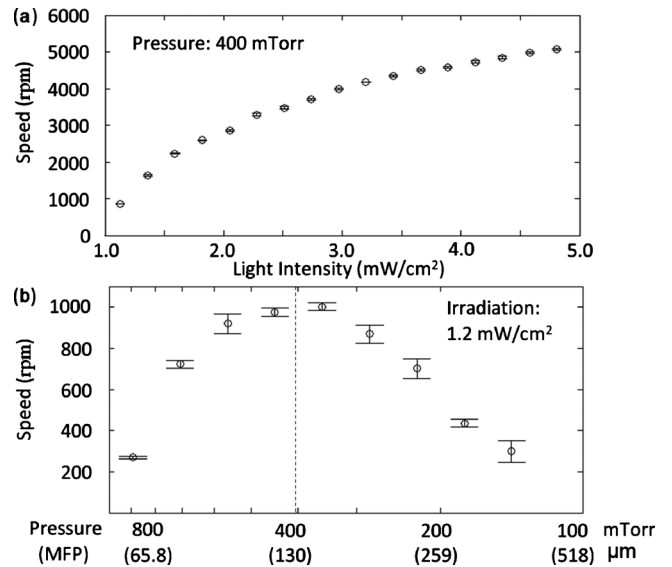


FIG. 3. Experimental data showing (a) light mill speed vs irradiation intensity at a constant pressure (400 mTorr) and (b) light mill speed vs pressure at a constant irradiation ($1.2 \text{ mW}/\text{cm}^2$). Each error bar indicates standard deviation of five measurements.

strongly at the wavelength near 540 nm,^{17,18} the absorption by close nanoparticles is drastically enhanced and expanded from the visible to near-infrared region (540–2000 nm); this enhancement stems from an electromagnetic interaction among the electrons at the surfaces of irradiated metallic particles.^{12,13} This electromagnetic interaction, which is known as plasmonic coupling effect, leads to accumulated electromagnetic energy in the spacing among nanoparticles, multiplying the light absorption by nanoparticles and by the gas molecules within interparticle spacing.¹⁹ Details about experimental and theoretical investigation of enhanced light absorption by fluidic molecules among close-packed metallic nanoparticles are given in our previous article.¹⁶ The density of accumulated photon energy (in watt per cubic meter) is

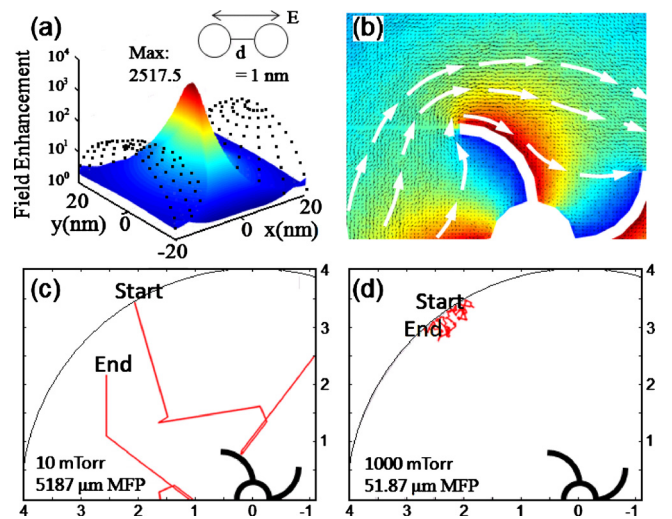


FIG. 4. (Color online) Different modeling results: (a) accumulation of photon energy among close gold nanoparticles with interparticle space equals 1 nm; the field enhancement shows the ratio of enhanced energy density to the incident light; the arrow indicates incident electric field; (b) heat-induced gas momentum at 400 mTorr (highlighted by white arrows); the color map indicates gas temperature (high and low); (c) simulated collisions encountered by a surrounding gas molecule at 10 mTorr; and (d) at 1000 mTorr; the unit of axes is mm; the circular boundary defines a isothermal wall at which gas temperature remains constant (at 25°C).

significant. For example, upon irradiation, the energy density in the interparticle spacing exceeds a hundred folds the energy density of incident light when the interparticle spacing is below 5 nm; this magnification exceeds 1000 folds when nanoparticles contact each other. Accordingly, besides receiving heat from the gold particles through heat transfer (conduction or radiation), gas molecules absorb photon energy directly from inside the interparticle spacing, which has high density of electromagnetic energy. The close-packed nanoparticles thus become an efficient light-powered heater for the surrounding gas molecules.

The light-driven motions of gas molecules are analyzed using molecular dynamics modeling for rarefied gas, the direct simulation Monte Carlo method. Detail about this modeling is in Refs. 20 and 21. The calculated result [Fig. 4(b)] shows that when a temperature gradient is established in the gas across the blade (with gas molecules at the convex side hotter than the concave side), this gradient generates a flow of heat-induced momentum (in kilogram meter per second) which forces the gas molecules to drive the light mill. At each individual blade, the flow of the induced momentum is from the concave (cooler) side to the convex (hotter) side. This result explains the observed rotating direction of the light mill (opposing the momentum flow) based on Newton's third law; the rotor is driven by a recoil momentum from the gas molecules.

To investigate the importance of temperature gradient across the blade, we used the same model for analysis upon a uniform cross-blade temperature, which equals the convex (hotter) side temperature from the previous simulation. The calculated result shows a weak and discontinuous momentum flow opposing the momentum flow from the previous simulation; the driving momentum induced by uniform heating on the blade is slightly against the observed rotation. This reversing effect is surpassed once the light-induced temperature gradient across the blade rises. This result shows that the shape-induced asymmetric photon heating at the blades is essential for the observed light mill rotation.

The effect of gas pressure to light mill rotation is investigated by molecular dynamics as well. The gas pressure determines the rate of collisions (in $1/\text{m}^3 \text{ s}$) among gas molecules. Under a low pressure, such as below 50 mTorr (MFP > 1 mm), a gas molecule may travel across the turbine experiencing no collision [Fig. 4(c)]. The molecule movement under such pressure is nearly random and is inefficient to develop a continuous momentum flow to sustain light mill rotation. Under a lower pressure, there are also fewer gas molecules to drive the light mill. Contrarily, when the pressure is higher than 1 Torr (MFP $\ll 75$ μm), frequent molecule collisions confine a gas molecule to a narrow region [Fig. 4(d)] and randomize the transport of heat-induced momentum, breaking the continuity of the induced momentum flow; the flow of momentum is especially discontinuous at the edges of blades, which are wider than the MFP of gas molecules. The optimized driving momentum takes place when the density of collisions is moderate; high enough to transport the momentum but low enough to yield sufficient mobility for gas molecules. The simulation shows that the pressure leading to optimized heat-induced momentum flow, which exerts maximized torque at the light mill, is about 400 mTorr (Fig. 5); the result is consistent with the experimental data.

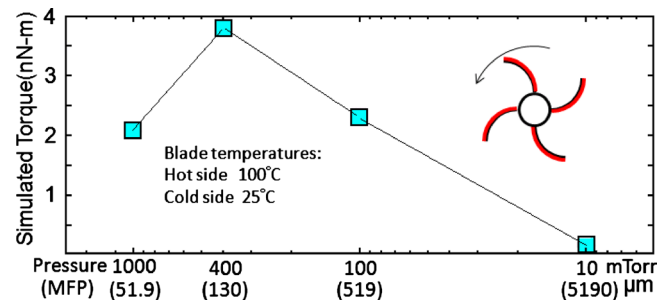


FIG. 5. (Color online) Simulated torque exerted by the circulating gas molecules at different gas pressures.

In summary, we have created a light mill with curled blades, which are homogeneously coated with dense nanoparticles for enhanced light absorption. This axially-asymmetric shape leads to asymmetric photon heating, creates a temperature gradient across the blade, and results in a forced circulation of the gas molecules that drive the light mill. The working principle of the light mill was investigated by molecular dynamics modeling, which gave results consistent with experimental data. The simplicity of this light mill promotes the development of light-powered motors of small dimensions, such as nanometer size. Nonetheless, larger light mills of same design can be developed for different applications, such as solar energy harvesting.

This work is supported by grants from the Office of Naval Research N00014-07-1-0609 and the National Science Foundation CMMI 0555275 to S.C. We appreciate the donation of the DMD tool kit from Texas Instruments. We also thank the computer support from Intel's High Education Program.

- ¹Y. Yu, M. Nakano, and T. Ikeda, *Nature (London)* **425**, 145 (2003).
- ²T. Muraoka, K. Kinbara, and T. Aida, *Nature (London)* **440**, 512 (2006).
- ³M. J. Madou, *Fundamentals of Microfabrication: The Science of Miniaturization* (CRC, New York, 2001).
- ⁴M. Ferrari, R. Bashir, and S. Wereley, *BioMEMS and Biomedical Nanotechnology* (Springer, New York, 2006).
- ⁵R. Osiander, M. A. G. Darrin, and J. Champion, *MEMS and Microstructures in Aerospace Applications* (CRC, Florida, 2006).
- ⁶A. Einstein, *Z. Phys.* **27**, 1 (1924).
- ⁷J. C. Maxwell, *Proc. R. Soc. London* **27**, 304 (1878).
- ⁸A. F. Fercher, W. Drexler, C. K. Hitzengerger, and T. Lasser, *Rep. Prog. Phys.* **66**, 239 (2003).
- ⁹M. D. Feldman, T. E. Milner, S. C. Chen, J. H. Kim, L. H. Han, J.-H. Oh, and H. Lee, U.S. Patent No. 7,711,413 (May 3 2010).
- ¹⁰See supplementary material at <http://dx.doi.org/10.1063/1.3431741> for the fabrication process.
- ¹¹S.M. Wu, L.H. Han, S.C. Chen, *Nanotechnology* **20**, 285312 (2009).
- ¹²D. W. Mackowski, *Proc. R. Soc. London, Ser. A* **433**, 599 (1991).
- ¹³R. Chern, X. Liu, and C. Chang, *Phys. Rev. E* **76**, 016609 (2007).
- ¹⁴S. Calvert and H. M. Englund, *Handbook of Air Pollution* (Wiley, New York, 1984), p. 103.
- ¹⁵D. Vokrouhlický, D. Nesvorný, and W. F. Bottke, *Nature (London)* **425**, 147 (2003).
- ¹⁶L. H. Han, W. Wang, Y. L. Lu, R. J. Knize, K. Reinhardt, J. R. Howell, and S. C. Chen, *ASME J. Heat Transfer* **131**, 033110 (2009).
- ¹⁷F. B. Craig and R. H. Donald, *Absorption and Scattering of Light by Small Particles* (Wiley, New York, 1983), p. 325.
- ¹⁸G. Mie, *Ann. Phys.* **25**, 377 (1908).
- ¹⁹J. D. Jackson, *Classical Electrodynamics*, 3rd ed. (Wiley, New York, 1999), pp. 309–313.
- ²⁰G. A. Bird, *Molecular Gas Dynamics* (Clarendon, Oxford, 1976), pp. 17–21.
- ²¹A. L. Garcia, *Numerical Methods for Physics* (Prentice-Hall, New Jersey, 1994), Vol. 47, p. 319.